



Anionic–cationic bi-cell design for direct methanol fuel cell stack

Hyea Kim, Murat Ünlü, Junfeng Zhou, Irene Anestis-Richard, Paul A. Kohl*

School of Chemical and Biomolecular Engineering, Georgia Institute of Technology, Atlanta, GA 30332-0100, United States

ARTICLE INFO

Article history:

Received 29 March 2010
Received in revised form 25 May 2010
Accepted 26 May 2010
Available online 31 May 2010

Keywords:

Direct methanol
Fuel cell
Anion conducting

ABSTRACT

A new fuel cell stack design is described using an anion exchange membrane (AEM) fuel cell and a proton exchange membrane (PEM) fuel cell in series with a single fuel tank servicing both anodes in a passive direct methanol fuel cell configuration. The anionic–cationic bi-cell stack has alkaline and acid fuel cells in series (twice the voltage), one fuel tank, and simplified water management. The series connection between the two cells involves shorting the cathode of the anionic cell to the anode of the acidic cell. It is shown that these two electrodes are at essentially the same potential which avoids an undesired potential difference and resulting loss in current between the two electrodes. Further, the complimentary direction of water transport in the two kinds of fuel cells simplifies water management at both the anodes and cathodes. The effect of ionomer content on the AEM electrode potential and the activity of methanol oxidation were investigated. The individual performance of AEM and PEM fuel cells were evaluated. The effect of ion-exchange capacity in the alkaline electrodes was studied. A fuel wicking material in the methanol fuel tank was used to provide orientation-independent operation. The open circuit potential of the bi-cell was 1.36 V with 2.0 M methanol fuel and air at room temperature.

© 2010 Elsevier B.V. All rights reserved.

1. Introduction

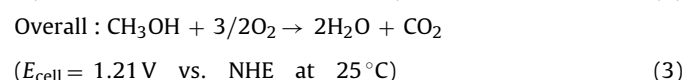
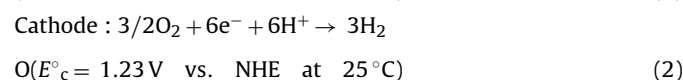
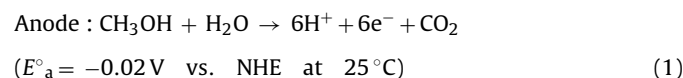
The development of high energy-density power sources for portable electronic devices is increasing. Direct methanol fuel cells (DMFCs) have several key advantages compared to other power sources. The high theoretical energy density of methanol (6100 Wh kg^{-1} at 25°C) may lead to small volume, long-life sources. The passive DMFC system, operating at atmospheric pressure and ambient temperature ($20\text{--}60^\circ\text{C}$), has a simple design, high energy efficiency, and minimal balance of plant. In addition, the liquid fuel is easy to store and handle.

In order to achieve higher voltage than values obtained from a single fuel cell, and high power-density, multiple fuel cells can be connected in series in a stack. Three different types of stack design for PEM fuel cell have been discussed [1–5]. The bipolar stack connects the anodes and cathodes in series through a metallic bipolar plate, which also serves as a fuel distribution channel. The second design is a monopolar stack where multiple anodes are serviced by the same fuel supply. The series connection is accomplished by electronically connected to the cathode of the next cell in a series configuration. Although it has attractive features, such as light weight and low cost, it was hard to achieve high power due to the high internal resistance [6,7]. Moreover, in case of DMFC application, there is a concern about possible electrolysis of the water in

the fuel, because more than 1.2 V could be produced with several electrodes sharing the same fuel tank.

Jiang and Chu [3] published a bi-cell stack design (or pseudo bipolar), as described in Fig. 1. Each unit consists of two PEM single cells. The two anodes (A_1 and A_2) operate with a common fuel source or channel, and the cathode (C_2) faces the cathode (C_3) in the next bi-cell unit. The anode (A_x) is electronically connected to the next cell's cathode (C_{x+1}) to form a series connection. It is easy to assemble the stack and the overall volume is smaller than the normal bipolar stack due to the common fuel tank. Also, the bi-cell design reduces the need for expensive bipolar plates.

However, there is a potential difference between anode A_1 and cathode C_2 . When these two electrodes are shorted together in the series configuration, the liquid methanol fuel provides an ionic path for anode A_1 to act as the anode to cathode C_2 . Since A_1 and C_2 are electrically shorted, no electrical current flows in the external circuit as a result of this electrochemical reaction. Under acidic conditions, the standard potential for the two electrochemical reactions is given in Eqs. (1) and (2), respectively, and the overall reaction is given by Eq. (3).



* Corresponding author. Tel.: +1 404 894 2893; fax: +1 404 894 2866.
E-mail addresses: Paul.Kohl@chbe.gatech.edu, kohl@gatech.edu (P.A. Kohl).

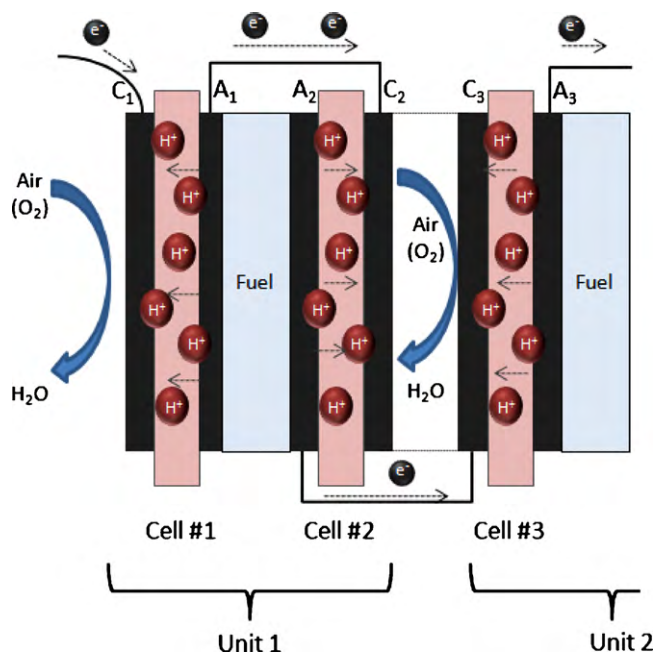
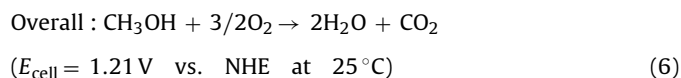
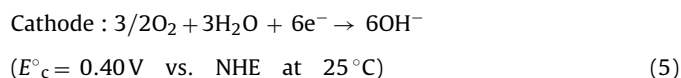
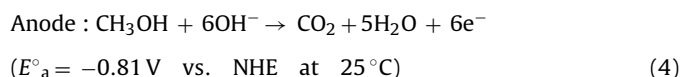


Fig. 1. A schematic of bi-cell stack design using PEM-PEM in series for H₂/air fuel cell. A: anode, C: cathode.

Thus, the origin of this electrochemical short circuit between anode A₁ and cathode C₂ is field developed between the electrodes and ionic path through the liquid methanol. This results in a self-discharge mechanism and loss of fuel efficiency. This same short circuit can also occur in the monopolar stack, since the anode in one cell is shorted to the cathode in the next cell and the two are ionically connected through the common methanol fuel tank. The magnitude of the undesired proton transport through the fuel tank could be lessened by spacing the cells farther apart or forming an insulating barrier between adjacent cells, however, this is at the expense of compact designs.

Recently, the development of anion exchange membranes (AEM) and anionic fuel cells has been reported [8–12]. Although AEM technology is not yet as mature as PEM (high ionic conductivity and stability of AEMs are still under investigation), AEM technology is promising because it could address several drawbacks with PEM fuel cell. The high pH environment in AEMFC provides faster kinetics for both oxygen reduction and methanol oxidation, which allows non-Pt catalysts such as silver and nickel to be used. The methanol crossover is expected to be lower due to the opposite direction of electro-osmotic drag.

In this paper, AEMs are used to improve the design and performance of the bi-cell stack. The fuel cell reactions for a DMFC with an AEM are shown in Eqs. (4)–(6).



In the alkaline fuel cell, the potentials are shifted to more negative values as a result of the high pH. This feature will be exploited in the study to improve the bi-cell design. The potential difference between the anode A₁ and cathode C₂ of the all PEM bi-cell design

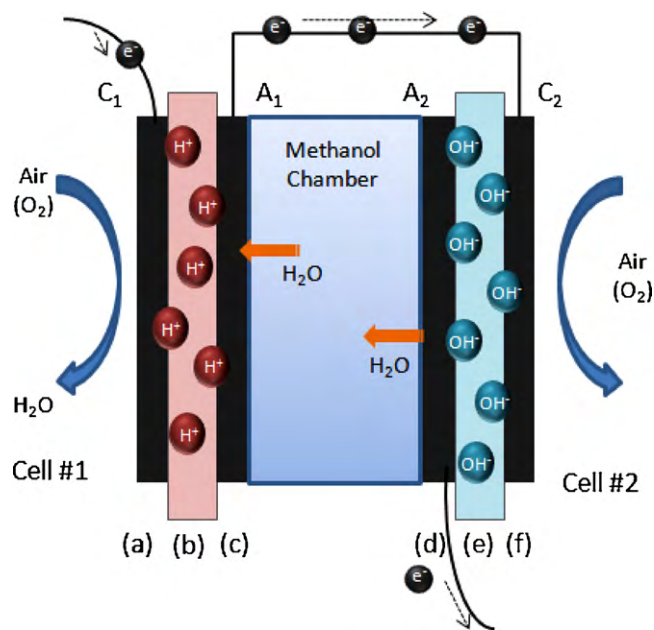


Fig. 2. A schematic of the AEM-PEM bi-cell stack for passive DMFC (PEM cathode (a), PEM (b), PEM anode (c), AEM anode (d), AEM (e), AEM cathode (f)).

can be changed by combining an AEM cell with a PEM cell as shown in Fig. 2. If cell #2 were changed from an acid cell to an alkaline one, then the cathode of cell #2 would be shifted to more negative potentials, as compared to the acid case (compare Eqs. (2) to (5)). The cathode of cell #2, C₂ is closer in potential to that of the anode of cell #1, A₁. Thus, the benefits of the alkaline-acid bi-cell design are explored in this paper. In addition, the electrode potentials of the alkaline design have been studied as a function of ionomer loading and methanol concentration. The performance of the PEM-AEM bi-cell has been investigated with a fuel wicking material, which is required for continuous fuel contact at different fuel tank orientations.

2. Experimental

The PEM electrode was made with Nafion ionomer (5 wt.% suspension), 40 wt.% Pt/C catalyst for cathodes, and 60 wt.% PtRu/C for anodes. The catalyst ink was prepared by mixing the catalyst, water (75 mg), Nafion ionomer and isopropyl alcohol (1:5 by mass of catalyst and ionomer to isopropyl alcohol). The catalyst ink was sonicated for 30 min and then sprayed onto hydrophobic carbon paper (TGPH-090) for the cathode, and hydrophilic carbon paper (2050L) for the anode. The electrodes had a surface area of 2 cm² and the metal loading was 4.0 mg cm⁻². Nafion 117 was pretreated with 3% H₂O₂, 1 M H₂SO₄, and water at 80 °C, each for 1 h. The electrode was pressed onto Nafion 117 at 2 MPa gauge pressure and 135 °C for 3 min.

The AEM electrode was made using an AEM ionomer, poly (arylene ether sulfone) functionalized with quaternary ammonium groups. The synthesis was described previously [9]. The physical properties of the AEM are summarized in Table 1. Two different ionomers with different ion-exchange capacity (IEC), L-AEM (low IEC AEM) and H-AEM (high IEC AEM), were used in this study. The AEM ionomer was diluted to 5 wt.% with dimethyl formamide (DMF). The catalyst ink for the AEM electrode was prepared by mixing the catalyst, water, AEM ionomer and a mixture of DMF (400 mg) and methanol (300 mg). The catalyst ink was sonicated for 30 min and sprayed onto the carbon paper, as described above for the PEM electrodes. Also, the resulting AEM electrodes had the

Table 1

Physical properties of the AEM membranes used in this study.

	L-AEM	H-AEM
DC ^a	0.8	1.2
Conductivity (mS cm ⁻¹)	14.0	23.0
Water-uptake (%)	48.0	63.9
Ion-exchange capacity (mmol g ⁻¹)	0.92	1.77

All measurements were made at room temperatures.

^a Degree of chloromethylation = number of chloromethyl groups/repeat unit, calculated from ¹H NMR spectra.

same surface area and metal loading as the PEM electrodes. Before fabricating a membrane electrode assembly (MEA), the AEM electrodes and membrane were immersed in aqueous 0.1 M KOH to exchange OH⁻ for Cl⁻. The AEM electrodes were then pressed onto the membrane at 0.5 MPa and 50 °F for 20 min. For half-cell MEA tests, a commercial Tokuyama AMX membrane was used. For performance test, H-AEM membrane was used and the membrane thickness was 140 μm.

The electrochemical experiments were performed with a PAR-STAT 2263 (Princeton Applied Research) potentiostat. Linear sweep voltammetry (LSV) was carried out with carbon cloth as a counter electrode and a saturated calomel (SCE) reference electrode (CH Instruments). In order to evaluate the effectiveness of the electrodes on the membranes in a fuel cell, an electrode was fabricated on one side of the membrane and tested as a half-cell in a three electrode configuration. A one sided electrode membrane assembly (half-MEA) was placed between the two glass cells and the electrode was a working electrode [13]. The counter and reference electrode were placed on the opposite side of the working electrode so that the protons produced traveled through the membrane, as they would in an operating fuel cell. The compartment on the membrane side containing the counter and reference electrodes was filled with the 1 M H₂SO₄ solution for PEM electrode and 1 M NaOH for the AEM electrode. The working electrode side was filled with concentrated methanol for anodes and air (or O₂) for cathodes. The potential was cycled at least 10 times at a scan rate of 10 mV s⁻¹ until steady state voltammometric behavior was obtained. Linear polarization was performed at a scan rate of 1 mV s⁻¹ and IR compensation was used to correct uncompensated resistance.

PEM and AEM single cells were fabricated for testing the fuel cell performance. The fuel cell hardware was made of graphite with small holes for fuel diffusion. The graphite was used as the current collector. The total exposed area was 0.3 cm². The current from the *I*-*V* polarization curves was reported without normalizing because of the difference in the electrode area (2 cm²) and the fuel exposed area. All MEAs were preconditioned by operating them as a fuel cell at a constant cell voltage of 400 mV for at least 2 h before performing *I*-*V* polarization experiments. The scan rate was 1 mV s⁻¹. All tests were performed at an ambient pressure and temperature.

3. Results and discussion

The electrode potentials of the AEM and PEM anode and cathodes were first investigated to examine the potential shift of the oxidation and reduction reactions with pH. The low pH electrode reactions were evaluated with an electrode fabricated with Nafion ionomer on a Nafion 117 membrane. The ionomer content was 30% of the mass of the carbon in the final dry electrode structure, which was previously optimized [14]. Fig. 3 shows the anode and cathode polarization curves for the PEM electrodes, as would occur in a PEM fuel cell. The potential of zero current for the reduction of oxygen from air was 0.91 and 0.95 V for the reduction of pure oxygen. This is approximately 0.3 V negative of the standard potential for oxygen reduction. The potential of zero current for methanol oxidation at the PEM anode was between 0.22 and 0.35 V. As the methanol

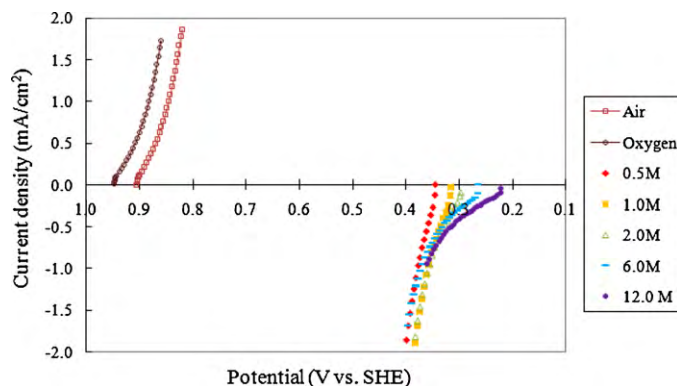


Fig. 3. Polarization curves of PEM anode with different methanol concentration and PEM cathode with air or oxygen.

concentration was increased from 0.5 to 12.0 M, the potential of zero current shifted to more negative values.

The anode and cathode polarization curves for the AEM electrodes were investigated in a similar manner as the PEM electrodes. Two half-cell MEAs were fabricated using commercial a Tokuyama AMX membrane and the high IEC ionomer, H-AEM. The ionomer content was 30 wt.% of the carbon in the final dry electrode structure. Fig. 4 shows the anode polarization curves under alkaline conditions, as in an AEM fuel cell for methanol concentrations of 1.0, 2.0 and 4.0 M. The onset of the oxidation of methanol occurred at about -0.5 V. This value is 0.8 V negative of the oxidation of methanol under acidic conditions at the PEM anode due to the shift in pH, as shown in Fig. 3. At higher methanol concentration, the potential of zero current shifted to more negative potentials, just as with the PEM anode. Concentrations higher than 4.0 M could not be used due to the solubility and swelling of the ionomer in the AEM samples. The potential of zero current for the reduction of humidified air and oxygen at the alkaline AEM cathode was 0.30 and 0.31 V, respectively. The values are within 0.1 V of the standard potential for oxygen reduction under alkaline conditions, Eq. (5).

Fig. 5 shows the current–voltage curves for the oxidation of 1 M methanol at the AEM and PEM electrodes, and the reduction of air at the AEM and PEM cathodes, plotted in one figure. The reduction of air at the AEM cathode is at essentially the same potential as the oxidation of methanol at the PEM anode. If used in a bi-cell configuration, where the high pH AEM air-cathode is shorted to the acid PEM anode, there is essentially no potential difference between the two electrodes, which mitigates the short circuit in an all-PEM bi-cell, as discussed in the introduction section.

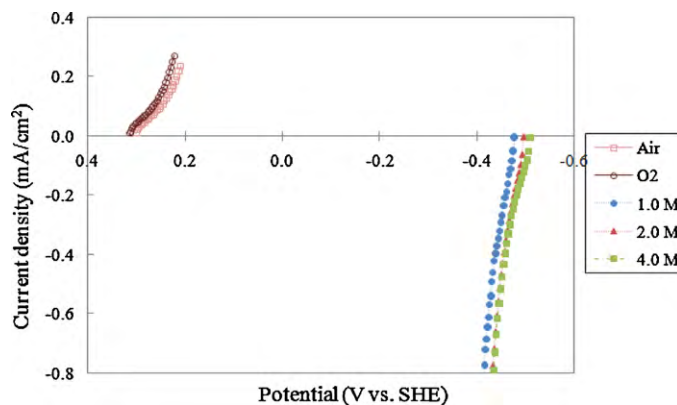


Fig. 4. Polarization curves of AEM anode with 1.0, 2.0 and 4.0 M methanol and AEM cathode with air or humidified oxygen.

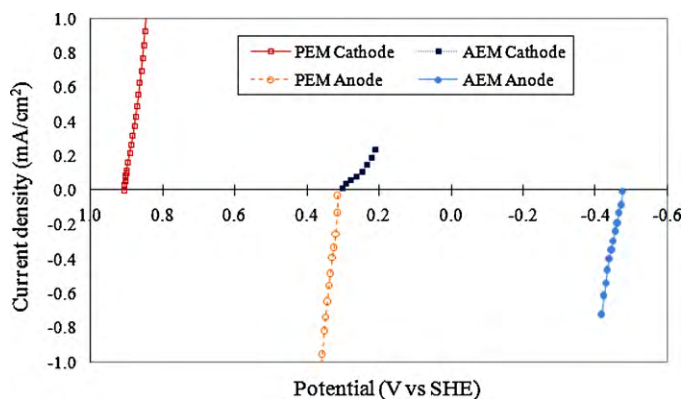


Fig. 5. Actual electrode polarization curves (AEM and PEM anode with 1.0 M methanol and AEM and PEM cathode with air).

On the other hand, Fig. 5 also shows one of the challenges facing high pH AEM based fuel cells. It is known that the kinetics for methanol oxidation and oxygen reduction in alkaline media are faster than in acid media [10,15]. However, the beneficial effects of alkaline media is not reflected in the current density for oxidation and reduction in alkaline media, compared to acid media in Fig. 5 due to the immature electrode fabrication technology for AEM electrodes. Advances in AEM electrode assemblies will improve the AEM fuel cell performance by decreasing the overpotential.

The effect of the ionomer content on the electrode potential of AEM anode was investigated. Fig. 6 shows that increasing the ionomer content from 10% to 50% shifted the potential of zero current to more negative values. The total hydroxide content and ionic pathway was increased with higher ionomer content inside of the electrode. However, when the ionomer content reached 70%, the potential of zero current shifted to more positive potentials. The methanol oxidation reaction occurs in the active surface area at the three-phase boundary of catalyst, reactant, and ionomer. With excess ionomer in the electrode, the reactants are obstructed from reaching the catalyst surface. Additionally in Fig. 6, there was a negative shift in the oxidation potential with higher methanol concentration.

The effect of ionomer content on the catalyst activity for methanol oxidation was also investigated. Fig. 7 shows the linear polarizations for methanol oxidation at the high pH AEM electrode as a function of the ionomer content. In this experiment, the same ionomer, H-AEM, was used to find the optimum content. An ionomer content of 30% was shown to yield the highest peak current for methanol oxidation at 0.15 V vs. SHE, which is near the operating point of an alkaline AEM fuel cell. The poor performance of the 10% ionomer content is likely due to the lack of an adequate three-

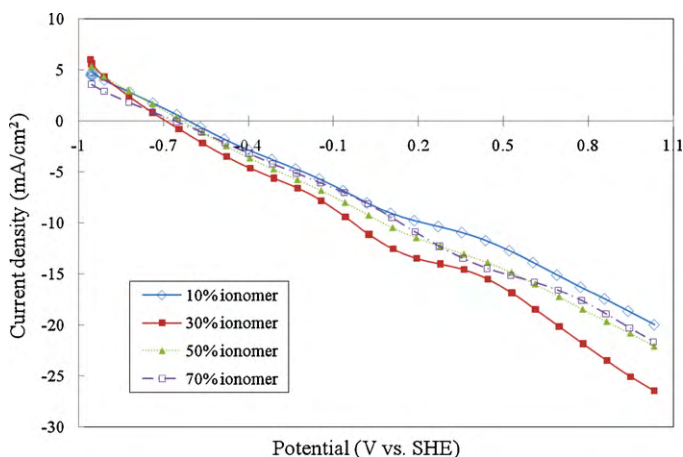


Fig. 7. Linear polarizations for methanol oxidation depending on ionomer content of H-AEM.

phase boundary. The poor performance at 50% and 70% ionomer was likely due to mass transfer limitations resulting in low catalyst activity [16–19].

Based on the optimized ionomer results shown above, an ionomer content of 30% was chosen for use in the electrodes for the alkaline, AEM fuel cell in the AEM-PEM bi-cell configuration. Fig. 8 shows the AEM fuel cell performance with the optimized ionomer content. The first AEM fuel cell was fabricated with H-AEM ionomer as the membrane and as the ionomer in the electrode assembly. A passive fuel cell configuration (i.e. stagnant tank of 2.0 M methanol) was as the fuel at the AEM anode. The AEM cathode was open to the ambient air at room temperature and ca. 40% relative humidity. The open circuit voltage of the cell was 0.57 V, and a current of 1.4 mA was measured at a cell voltage of 0.4 V. In order to compare cell performance for electrodes with different ionomer content, a second AEM fuel cell was prepared with the lower IEC ionomer, L-AEM. The membrane electrode assembly had the same membrane as the first fuel cell, H-AEM. It was found that the L-AEM ionomer led to higher fuel cell performance, Fig. 8. The open circuit voltage was 0.64 V and the current was 3.28 mA at 0.4 V. This is twice the current achieved with the H-AEM ionomer. Since H-AEM has a higher ionic conductivity and IEC, as shown in Table 1, it is clear that the microstructure and water swelling in the electrode assembly are critical factors, rather than simply ionic conductivity. The L-AEM ionomer has less water swelling due to its lower quaternary ammonium density than the H-AEM ionomer, which is the most likely cause of the performance difference between the two ionomers. It is common for membranes with a high degree of

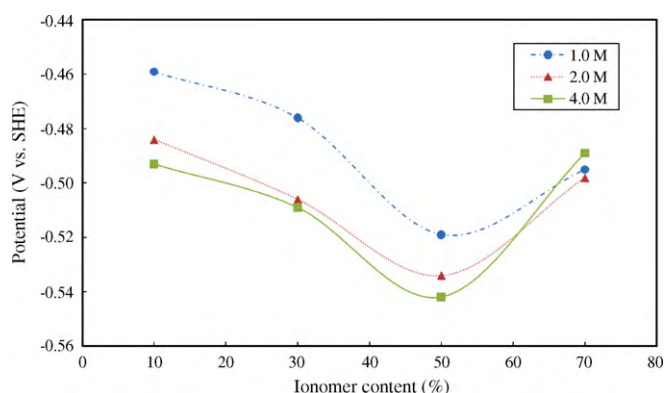


Fig. 6. AEM anode OCV depending on ionomer content and methanol concentration.

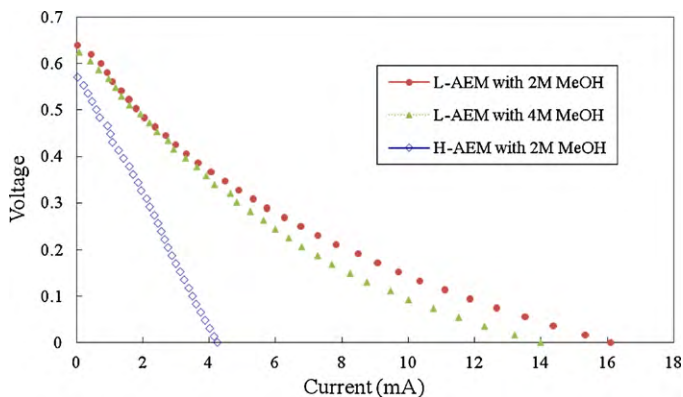


Fig. 8. AEMFC performance with H-AEM membrane and different IEC ionomers, L-AEM and H-AEM, at room temperature.

chloromethylation, and resulting quaternary ammonium content, to have higher conductivity and IEC, but also higher water-uptake [9]. High water-uptake can result in flooding in the electrode which can impede the mass transfer of reactants inside the catalyst layer.

The AEM fuel cell was also tested in 4.0 M methanol with the L-AEM electrode assembly, as shown in Fig. 8. Since there is no pressure difference across the membrane in a passive system (the fuel is not pumped to the anode), a higher methanol concentration can lead to higher performance, unless other factors, such as cross-over, become a factor [20]. In this case, the performance of the L-AEM ionomer with 4.0 M methanol fuel was slightly worse (open circuit voltage of 0.67 V) than the 2.0 M methanol case.

Maintaining electrode-fuel contact is critical in liquid feed fuel cells, especially for portable devices which can be moved and rotated. Thus, it is desirable to use a wicking mechanism to keep the electrode assembly wet with fuel even when the device is inverted. This concern is especially true in the bi-cell configuration, as shown in Fig. 2, where the two electrodes are mounted opposing each other. In the AEM-PEM bi-cell configurations assembled here, hydroxy-methoxy cellulose (HMC) was used in the fuel tank as a liquid wicking material. The single fuel cell performance with HMC was tested at different orientations: anode-side up, upside down and a 90° angle. Steady state performance was achieved at all three orientations, however, it is of interest to evaluate the performance under wicking conditions vs. no wicking conditions. Thus, the single fuel cell performance in 2 M methanol was tested with or without HMC. It was found that the AEM fuel cell performance was same in all cases. Interestingly, the PEM fuel cell performance changed when HMC was used, as shown in Fig. 9. The open circuit voltage of the PEM fuel cell was 0.1 V higher with HMC. The most likely cause of the improved performance was a decrease in cross-over with HMC due to the flow restrictions HMC causes [21]. The methanol cross-over in an AEM cell is lower than in a PEM cell because electro-osmotic is in the opposite direction. If a higher concentration of methanol (>2 M) was used, the effect of fuel restriction by the HMC on the AEM cell is expected to be the same as the PEM case.

Finally, the AEM-PEM bi-cell was constructed. An o-ring style glass joint was used to construct the fuel reservoir between the AEM and PEM fuel cells. The AEM and PEM fuel cells were 5 cm apart and the two anodes shared the common methanol fuel tank which included the HMC. Each cathode was open to the air on the outside of the assembly. The cells were operated at room temperature and humidity (ca. 40% relative humidity). The AEM cathode was shorted to the PEM anode. It was confirmed that there was no current flow between the AEM cathode and PEM anode. In a separate experiment, two PEM cells were used in the same bi-cell configuration, Fig. 1. A small current of 4 μ A was observed between the anode #1 and cathode #2 (the electrode size was 2 cm²), which indeed

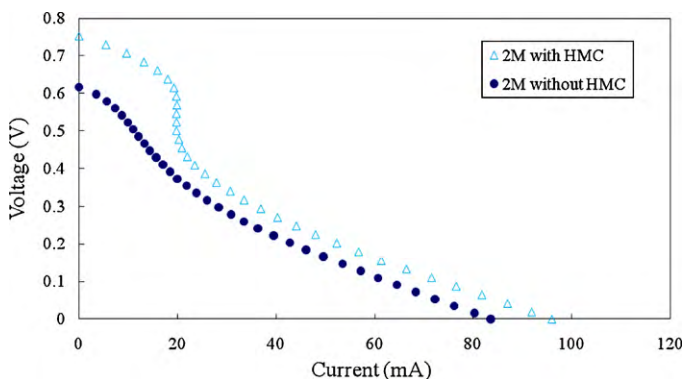


Fig. 9. The effect of HMC on PEMFC performance prepared using Nafion 117 membrane and Nafion ionomer.

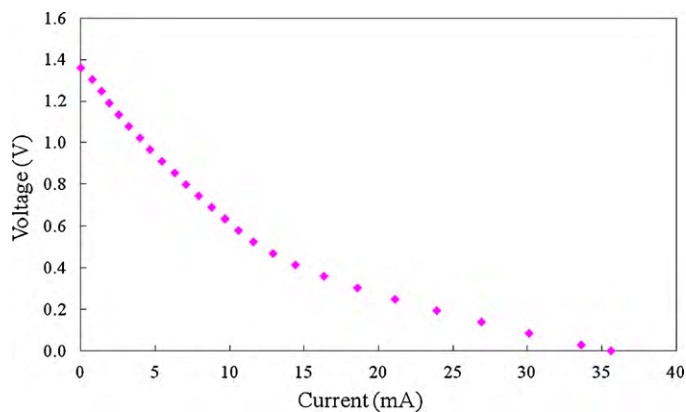


Fig. 10. The bi-cell performance with 2 M methanol and air at room temperature.

showed the expected short circuit current discussed in Section 1.

Fig. 10 shows the performance of the AEM-PEM bi-cell, which is composed of the PEM cell from Fig. 9 and AEM cell from Fig. 8 (using L-HMC ionomer in the electrodes). The open circuit voltage of the bi-cell at ambient temperature and relative humidity was 1.36 V, which corresponds to the sum of the open circuit voltages of the AEM and PEM cells. The current was 7.1 mA at 0.8 V. The moderate performance of the current bi-cell system is limited by the performance of the less mature AEMFC. The bi-cell performance will be increased as the AEM cell technology improves and better matches that of the PEM technology, including the membrane development with high conductivity and stability. The performance here does serve as a demonstration of the advantages of the mixed acid-alkaline bi-cell construction.

In addition to the common-voltage AEM cathode/PEM anode configuration, there are several other intriguing aspects of the bi-cell design in the area of water management. As shown in Eqs. (2) and (5), water is produced at the PEM cathode and AEM anode, respectively. This complementary water generation and consumption feature of the AEM and PEM technology can be used to provide self-humidification and water management. That is, an air stream flowing across alternating AEM and PEM cathodes will be alternately humidified and dehumidified. Likewise, the methanol fuel will be become diluted by water entry from the AEM cell and depleted of water by the PEM cell. A detailed analysis of electro-osmotic drag and other factors is now underway to better understand these features.

4. Summary

Three different types of stack design for fuel cells have been discussed. The bipolar stack is the most common design due to the high fuel cell performance, even though the metallic bipolar plate is expensive. The monopolar stack has the advantage of light weight and low cost. The bi-cell stack could reduce the overall system volume due to the use of a common fuel tank. However, the fuel cell performance of the monopolar and bi-cell stack is lower than the bipolar configuration due to the high internal electrode resistance from the wire connection because a metallic current collector cannot be used. Also, in the case of the DMFC application, there exists the possible ionic short circuit between adjacent anodes through the common fuel tank. In order to address this concern, a bi-cell design with an AEM and PEM fuel cell in series using a common liquid fuel tank was demonstrated. The electrode potentials for both acid – PEM and alkaline – AEM were evaluated and shown to match the combined cell. The actual AEM cathode potential was essentially the same as the PEM anode potential making the bi-cell configuration viable. High ionomer content was shown to cause a

negative shift in anode potential of zero current. A 30% loading of the H-AEM ionomer was found to be the optimum content for the current AEM fuel cell. The performance of AEM fuel cell prepared with the L-AEM ionomer showed higher performance than that of the H-AEM ionomer due to lower water-uptake. Fuel wicking with HMC was shown to help achieve orientation-independent performance. The bi-cell system was demonstrated with the optimized AEM and PEM fuel cell in series operated from a single fuel tank. In addition to the higher voltage (theoretically, 2.4 V) and reduced volume using a common fuel tank, self-humidification and easy water management are interesting advantages of the AEM–PEM bi-cell stack.

References

- [1] D. Chu, R.Z. Jiang, J. Power Sources 80 (1999) 226–234.
- [2] A. Heinzl, C. Hebling, M. Muller, M. Zedda, C. Muller, J. Power Sources 105 (2002) 250–255.
- [3] R.Z. Jiang, D.R. Chu, J. Power Sources 93 (2001) 25–31.
- [4] Y.J. Kim, B. Bae, M.A. Scibioh, E. Cho, H.Y. Ha, J. Power Sources 157 (2006) 253–259.
- [5] M. Oszcipok, M. Zedda, J. Hesselmann, M. Huppmann, M. Wodrich, M. Jung-hardt, C. Hebling, J. Power Sources 157 (2006) 666–673.
- [6] D.J. Kim, E.A. Cho, S.A. Hong, I.H. Oh, H.Y. Ha, J. Power Sources 130 (2004) 172–177.
- [7] D. Kim, J. Lee, T.H. Lim, I.H. Oh, H.Y. Ha, J. Power Sources 155 (2006) 203–212.
- [8] J.R. Varcoe, R.C.T. Slade, G.L. Wright, Y.L. Chen, J. Phys. Chem. B 110 (2006) 21041–21049.
- [9] J.F. Zhou, M. Unlu, J.A. Vega, P.A. Kohl, J. Power Sources 190 (2009) 285–292.
- [10] J.R. Varcoe, R.C.T. Slade, Fuel Cells 5 (2005) 187–200.
- [11] J.R. Varcoe, R.C.T. Slade, E.L.H. Yee, S.D. Poynton, D.J. Driscoll, D.C. Apperley, Chem. Mater. 19 (2007) 2686–2693.
- [12] M.Ü.J.F. Zhou, I. Anestis-Richard, P.A. Kohl, J. Membr. Sci. 350 (2010) 7.
- [13] H. Kim, P.A. Kohl, J. Power Sources 195 (2010) 2224–2229.
- [14] E. Antolini, L. Giorgi, A. Pozio, E. Passalacqua, J. Power Sources 77 (1999) 136–142.
- [15] E.R.G.E. Antolini, J. Power Sources 195 (2010) 20.
- [16] H. Bunazawa, Y. Yamazaki, J. Power Sources 182 (2008) 48–51.
- [17] J.H. Kim, H.Y. Ha, I.H. Oh, S.A. Hong, H.N. Kim, H.I. Lee, Electrochim. Acta 50 (2004) 801–806.
- [18] B. Krishnamurthy, S. Deepalochani, K.S. Dhathathreyan, Fuel Cells 8 (2008) 404–409.
- [19] J.S. Lee, K.I. Han, S.O. Park, H.N. Kim, H. Kim, Electrochim. Acta 50 (2004) 807–810.
- [20] J.G. Liu, T.S. Zhao, R. Chen, C.W. Wong, Electrochem. Commun. 7 (2005) 288–294.
- [21] S.K. Kamarudin, W.R.W. Daud, S.L. Ho, U.A. Hasran, J. Power Sources 163 (2007) 743–754.